ISSN 0145-8752, Moscow University Geology Bulletin, 2015, Vol. 70, No. 2, pp. 141–151. © Allerton Press, Inc., 2015.
Original Russian Text © E.Yu. Baraboshkin, A.Yu. Guzhikov, V.N. Benyamovsky, G.N. Aleksandrova, E.E. Baraboshkin, A.M. Surinsky, 2015, published in Vestnik Moskovskogo Universiteta. Geologiya, 2015, No. 2, pp. 68–77.

New Data on the Stratigraphy and Environment of the Eocene Formation at the Aktolagay Plateau (West Kazakhstan)

E. Yu. Baraboshkin[a], A. Yu. Guzhikov[b], V. N. Benyamovsky[c], G. N. Aleksandrova[c], E. E. Baraboshkin[a], and A. M. Surinsky[b]

[a]*Department of Geology, Moscow State University, Moscow, 119991 Russia*
[b]*Saratov State University, Saratov, Russia*
[c]*GIN RAS, Moscow, Russia*
e-mail: barabosh@geol.msu.ru, aguzhikov@yandex.ru, vnben@mail.ru, dinoflag@mail.ru, baraboshkin_zhen@mail.ru, arsur91@yandex.ru

Received November 10, 2014

Abstract—Detailed geological description along with sedimentological and petromagnetic studies provided new data on the structure and formation environments of the Eocene key section at the Aktolagay Plateau (North Peri-Caspian, West Kazakhstan). The volumes of the Alashen and the Tolagaysor Formations were revised.

Keywords: Eocene, Ypresian Stage, stratigraphy, magnetostratigraphy, petromagnetism, sedimentology, trace fossils, Aktolagay Plateau, West Kazakhstan, Nothern Peri-Caspian

DOI: 10.3103/S0145875215020027

INTRODUCTION

The first brief mention of the Paleogene (Eocene) section at the Aktolagay Plateau (obsolete spelling Aktulagay) southwest of the Aktube district on the left bank of the Emba River in its middle course in West Kazakhstan, Fig. 1) was published in *The Geology of the Soviet Union* (1970). The section is exposed at an eponymous salt dome (N 47°32′29.9″, E 55°09′12.3″); it is well known through publications due to its good exposures, considerable completeness of the section and its good characterization by complexes of shark teeth (Beniamovskiy, 1994; Zhelezko and Kozlov, 1999; Malyshkina, 2006; Steurbaut, 2011; King et al., 2013). The section represents the type sections of the Alashen and the Tolagaysor Formations (Beniamovskiy et al., 1990). In 2013 the section (observation point 3020) was studied in detail and thoroughly sampled by the "sample-in-sample" technique. Samples for macrofossils (shark teeth), microfossils (foraminifers, nano-plankton, and pollen) and oriented samples for magnetostratigraphic studies have been collected at 75 levels. As well, samples for petromagnetic studies were taken at 218 (about at every 0.3 m) troughs over all of the ~73 m of the section's total thickness. The data on sedimentology and petromagnetism obtained up to the present permit detailed subdivision of the section, clarifying demarcation of the Formations and allowing reconstruction of some features of sedimentation.

THE STRUCTURE OF THE SECTION

The section rests on an extensively eroded white chalk member penetrated by *Thalassinoides* burrow roofs of the Maastrichtian. The following sequence is observed (from the bottom upward, Fig. 2, 3).

The Alashen Formation, Lower Sub-Formation

Unit 1 (samples 2–9). Greenish-gray plastic clay at the very bottom (Unit A1, after King et al., 2013) and in upper part faintly laminated, slightly calcareous, bioturbated by large *Chondrites targionii* (Brongn.) along with small *Ch. intricatus* (Brongn.) (Fig. 3, 3), with limonitized (after pyrite) *Pilichnus dichotomus* Uchman, less often *Planolites*. In the lower part the clay is finely laminated, practically without bioturbation. Fish remnants and scarce bivalves occur. The base of the unit is sharp with gypsum crust and Fe hydroxides along it (Fig. 3, 7), with greenish clayey sands occurring above it. The latter contains fine pebbles and gravel of limestone, phosphorite and phosphatized shark teeth. The same sediments fill small erosion cavities and *Thalassinoides* burrows (Fig. 3, 7) that descend for 50–60 cm into the roof of the Maastrichtian. In some places erosion cavities preserve the deposits of the Upper Paleocene (ibid.). The Unit is 8.5 m thick.

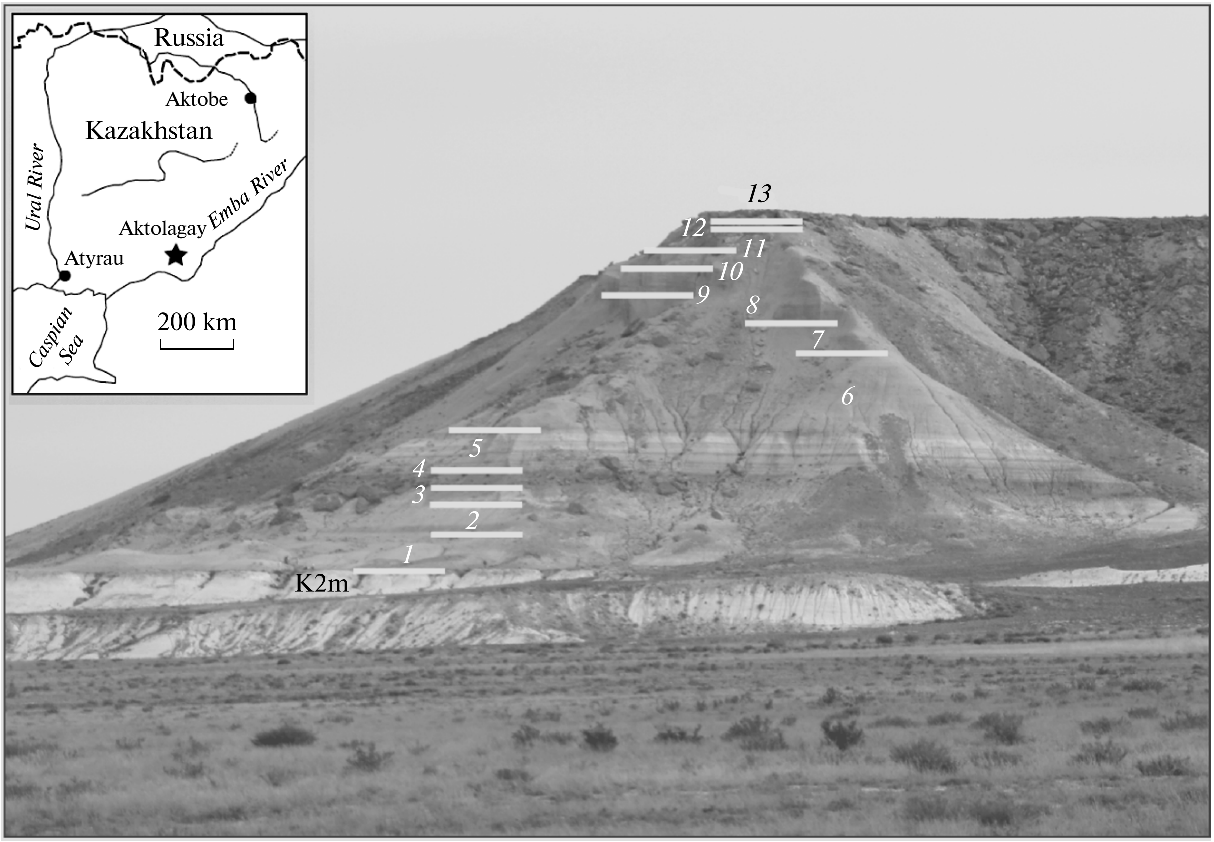

Fig. 1. A map of the location of the section (insert) and a general view of the studied key section with the positions of the recognized Units.

The Alashen Formation, Middle Sub-Formation

Unit 2 (samples 10–14). Greenish-gray calcareous clay with horizontal bedding at the bottom (0.7–1.1 m) and bioturbated in the upper part. The thickness is 4.1–4.4 m.

Unit 3 (samples 15–20). The rhythmic interbedding of greenish-gray bioturbated and dark finely-laminated clays and shales occurs. The trace fossils are *Pilichnus dichotomus* Uchman, *Planolites* and *Chondrites intricatus* (Brongn.) (Fig. 3, 1). King et al. (2013) also reported the presence of *Thalassinoides* and *Zoophycos*. The mass presence of *Chondrites intricatus* (Brongn.) filled by both light and dark clays occur at certain levels that mark short hiatuses (omission surfaces after King et al., 2013). Fish remnants and bivalve shells are scarce. The thickness of the unit is 10.3 m.

Unit 4 (samples 21–23). Rhythmic interbedding of finely laminated dark-brown bituminous shale (0.3–0.8 m) and brownish-grey shale-like clays (0.2–0.3 m, Fig. 3, 5). The thickest (0.8 m) of the upper layer of the slate has an eroded roof. No bioturbation was observed. Fish remnants are abundant. Gypsum–limonite (after pyrite) concretions occur. The total thickness is 3.1 m.

The Alashen Formation, Upper Sub-Formation

Unit 5 (samples 24–32). Rhythmic interbedding of dark–brown bioturbated bituminous shale (0.1–0.5 m) and greenish clay (0.2–2.1 m) (Fig. 3, 5). The clay thickness considerably increases up the sequence. The trace fossils are *Chondrites intricatus* (Brongn.), sparsely by *Planolites* (Fig. 3, 4). *Chondrites intricatus* (Brongn.) occurs abundantly along certain levels with hiatuses, which was also reported by King et al. (2013). At the base of the Unit there are some erosional surfaces that are pronounced to various extents: at these surfaces numerous fine (1–3 cm) phosphorites occur, some of these are phosphatized coprolites *Lumbricaria intestinum* Münst., *L. gordialis* Münst., bones and vertebra of fish, and shark teeth (Fig. 3, 6). Some gypsum–limonite (after pyrite) concretions occur as well: those practically disappear in the upper part of the Unit. The top of the Unit is eroded. The thickness is 8.7 m.

The Tolagaysor Formation

Unit 6 (samples 33–47). Interbedding of cm-thick layers of greenish-grey and brownish faintly bedded silty clays and mm-thick layers and lenses of fine-grained sands and siltstones. At the Unit's bottom in cm-thick sand layers cross-bedding is observed. In the 5 upper meters of Unit 6 the silt proportion notably decreases. Isolated bioturbations in the sediments are represented by *Chondrites* isp., and *Skolithos* isp. Limonitized pyrite concretions are few in number. The thickness of the Unit is 15.4 m.

Unit 7 (samples 48–52). Greenish-grey and brownish faintly and horizontally laminated clays with sparse mm-sized layers of silt. The Unit is 9.5 m thick.

Unit 8 (samples 53–57). The rocks are similar to those from Unit 6, but contain a few horizons of carbonate concretions up to 10–15 cm in size. The thickness is 4.1 m.

Unit 9 (samples 58–62). The rocks are similar to those from Unit 6, but with a higher proportion of silt and contains numerous scattered limonite (after pyrite) concretions and scarce *Chondrites* isp. The thickness is 5.9 m.

Unit 10 (samples 63–67). Greenish-grey almost pure laminated plastic clays with a minor proportion of silt. As well, siderite concretions occur, fine grains of glauconite and bivalve shells (King et al., 2013). The roof is eroded. The thickness is 4.3 m.

The Sangryk Beds

Unit 11 (samples 68–72). Laminated dark-brown bituminous shale. In the upper 1.5 m of the Unit the shales are greenish-grey in color and show traces of slide deformations (Figs. 3, 8). A layer of siltstone occurs at the bottom of the Unit: it contains well-rounded pebbles of cherty and phosphorite sandstones (up to 4 cm in diameter), as well as phosphatized remains of large bones of vertebrates and shark teeth. The roof of the Unit is eroded. The total thickness is 5 m.

The Sarmatian Stage

Units 12–13 (samples 73–75). In the base of the Unit yellow loose sands up to 1 m occur as thick with interclasts of clays and quartz pebbles from the base of which vertical burrows of *Ophiomorpha* protrude. The sands are overlain by bioclastic platy limestones (1.2–1.5 m as thick): they contain a clastic admixture with large-scale trough bedding and bedding of the "fish

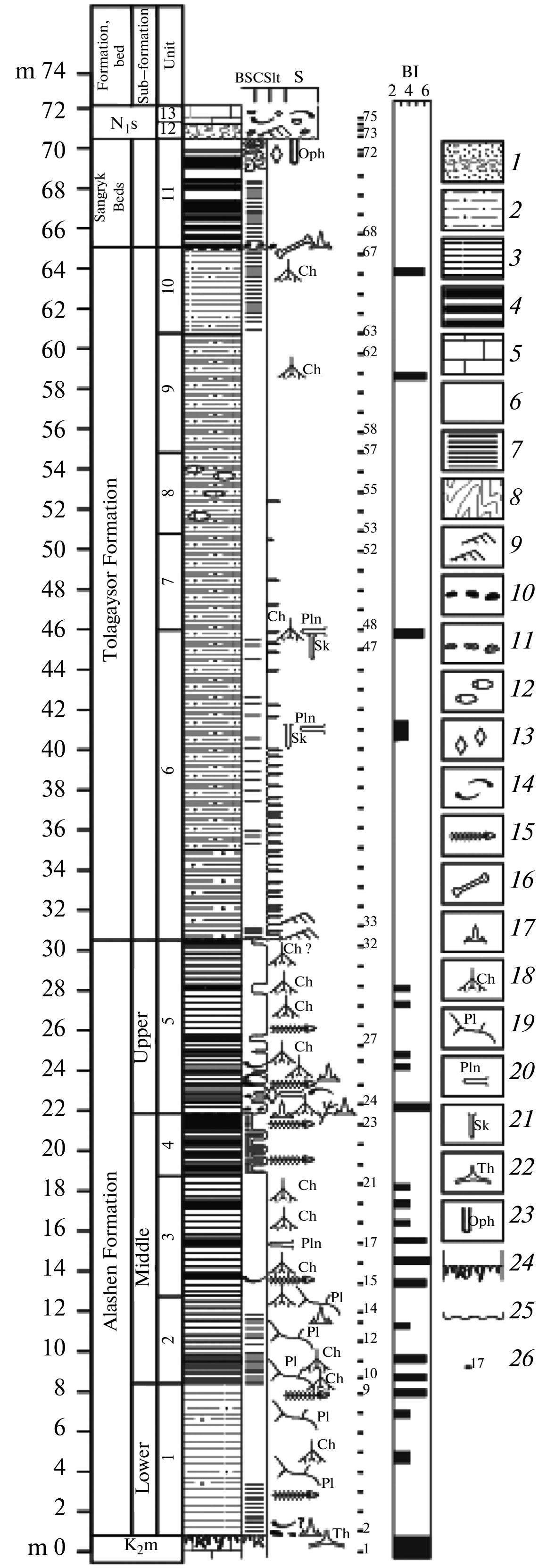

Fig. 2. The structure and bioturbation intensity of the section: rocks: *1*, sands (S) with pebbles; *2*, siltstone (Slt); *3*, clays (C); *4*, bituminous shales (BS); *5*, limestones; textures: *6*, massive; *7*, horizontally beded; *8*, landslide; *9*, cross, bedding; other elements of the section: *10*, phosphorite pebbles; *11*, interclasts; *12*, calcareous concretions; *13*, gypsum crystals; fossils: *14*, mollusks; *15*, fish; 16, large vertebrates; *17*, shark teeth; bioturbations: *18*, *Chondrites*, *19*, *Pilichnus*, *20*, *Planolites*, *21*, *Skolithos*, *22*, *Thalassiniodes*, *23*, *Ophiomorpha*; boundaries: *24*, hard bottom; *25*, erosional; *26*, sampling locations and their numbers (only mentioned in the text and shown in the figures). BI, bioturbation index, after Droser and Bottjer (1986).

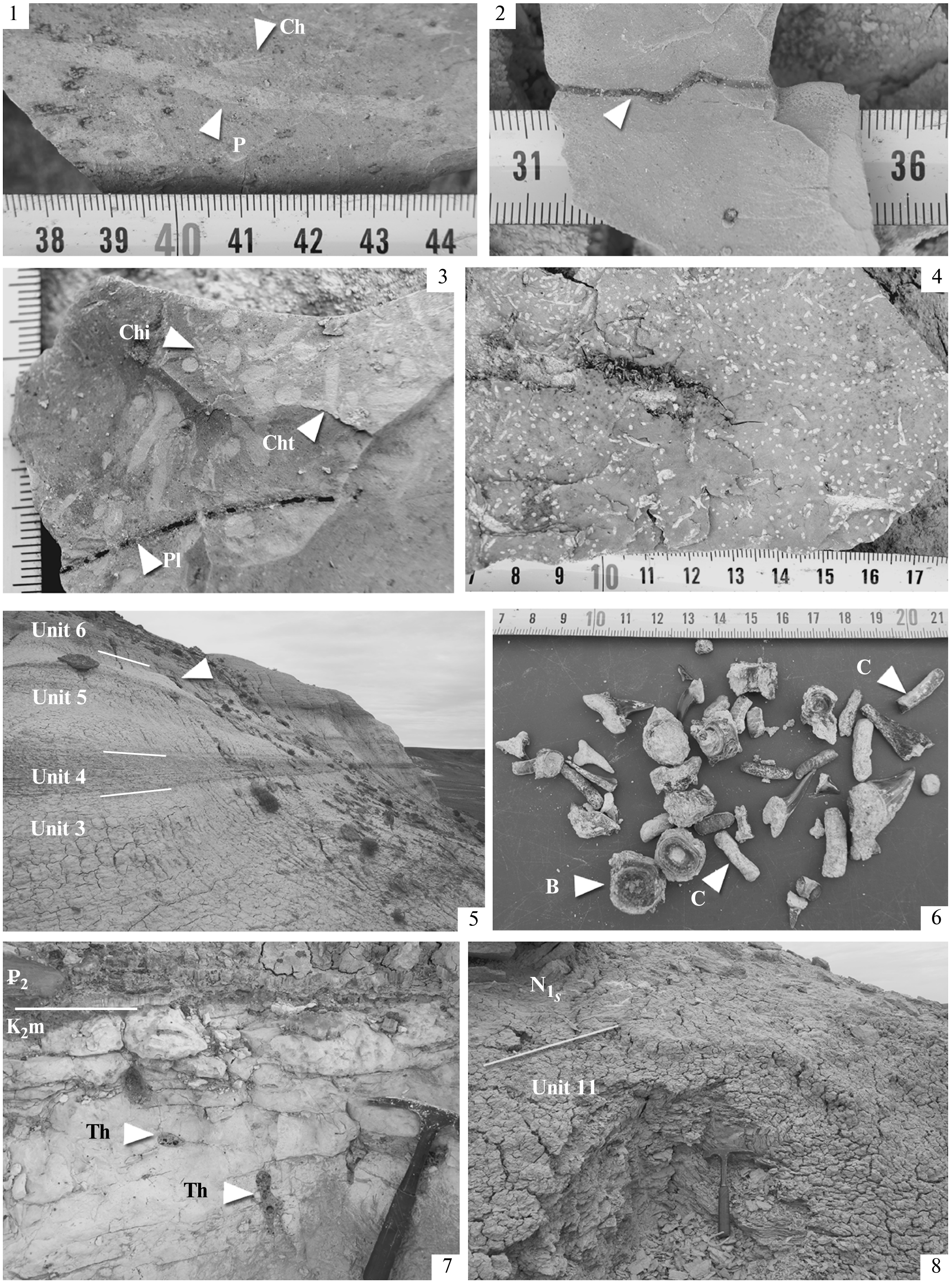

Fig. 3. Ichnofossils and the characteristics of the section's structure: 1, burrows of *Planolites* (P) and *Chondrites intricatus* (Brongn.) (Ch) in Unit 3 clays (sample 17); 2, pyritized burrow of *Pilichnus* in Unit 2 clay (sample 10); 3, burrows of *Chondrites targionii* (Brongn.) (Cht), *Ch. intricatus* (Brongn.) (Chi) and pyrite, substituted *Pilichnus dichotomus* Uchm. (Pl) from Unit 1 (sample 9); 4, numerous *Chondrites intricatus* (Brongn.) from base of Unit 5 (sample 24); 5, general view of the middle (Units 3 and 4) and upper (Unit 5) subformations of the Alashen Formation and base (Unit 6, arrow) of the Tolagaysor Formation; 6, phosphatized coproliths (C) fish vertebras (B) and shark teeth from the base of Unit 5; 7, boundary of the Maastrichtian and Eocene (Unit 1) 6 km south–southwest from the studied section: Th, *Talassinoides* burrows with fine pebbles and gravel of Paleocene, Eocene limestone and phosphorite; 8, landslide deformations in the bituminous slates, Unit 11, below the Miocene sediment base.

bone" type, which cover the surface of the plateau. The visible thickness is 2.5 m.

RESULTS AND DISCUSSION

Lithostratigraphic Studies

Beniamovskiy et al. (1990) described stratotypes of the Alashen and Tolagaysor Formations in this section (Table 1). The boundary between them was established at the base of shales of Unit 4, while the roof of the Tolagaysor Fm. occurs in the base of clays of Unit 12, which is ascribed by the mentioned authors to the Sarmatian Stage.

Later, Zhelezko and Kozlov (1999) included shales of Unit 11 in the Tolagaysor Formation, while only overlying limestone was ascribed to the Sarmatian Stage (Table 1). The attribution of the clays of Unit 11 to the formations was not determined, although in a similar interval at South Emba the Keresta Formation was described. In the middle reaches of the Emba River the new Sangryk Unit was introduced (ibid). It is notable that earlier this interval in the Utvinsk–Khobdinsk district was ascribed to the Shubarsay Formation (Beniamovskiy, 1994).

In publications by Steurbaut (2011) and King et al. (2013) the Alashen Formation was described in an earlier volume: the shales of Unit 4 were recognized as the new Aktulagay Formation. The volume of the Tolagaysor Formation's was reduced to Units 6–10 while Unit 11 was correlated with the Sangryk Unit, although its rank was elevated up to formation without proper argumentation (Table 1).

Description of the Aktulagay Formation in the studied section is not correct, since such a formation was earlier described in the Senomanian deposits of Aktolagay Plateau (Koltypin, 1957).

On the basis of analysis of complex of the litho- bio- and magnetostratigraphic data the volumes of the formations were revised. We suggest that the lower part of the section (Units 1–5), which is represented by regular interbedding of calcareous clays and bituminous shales or shale-like clays, was accumulated during a single stage of development of the anoxic basin and corresponds to the Alashen Formation. This formation is subdivided into three sub-formations: the lower (Unit 1) contains layers of slaty clays, bioturbated by *Chondrites*. The middle sub-formation (Units 2–4) begins with thick layer of horizontally bedded calcareous slaty clays, corresponding to an increase of anoxic conditions. Unit 3, which corresponds to the beginning of the anoxic environment contains thin beds of true bituminous shale (sapropelites) bioturbated by *Chondrites*. The thickest sapropelites of Unit 4 were formed during significant anoxic conditions and bear no traces of bioturbation. The upper sub-formation (Unit 5) separated by the erosion surface of the hiatus with phosphorite is represented by rhythmic interbedding of bioturbated dark-brown bituminous shales and

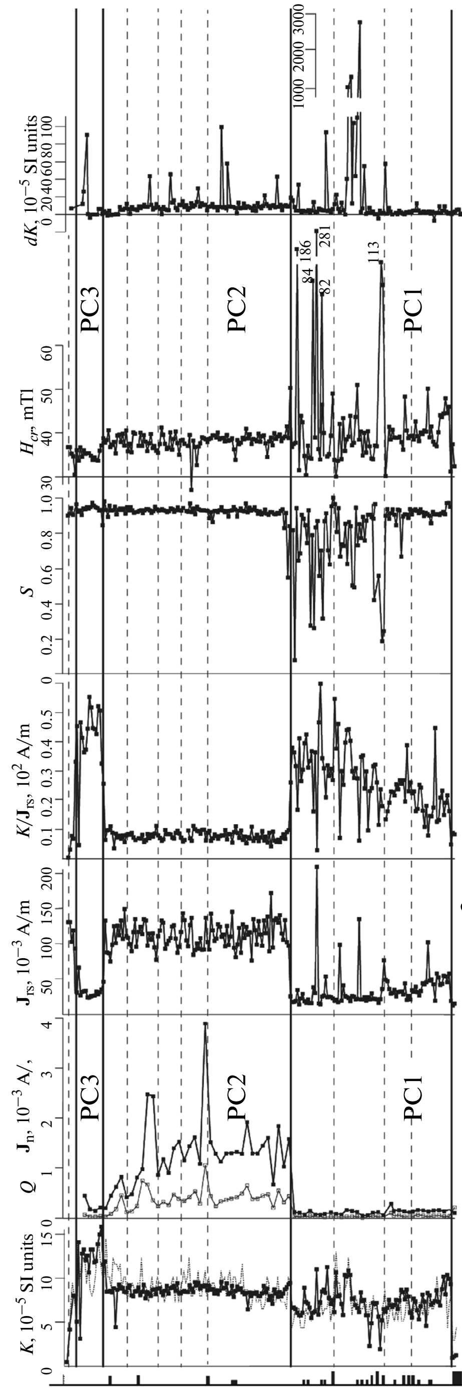

Fig. 4. The petromagnetic section of the Eocene sediments of the Aktolagay Plateau (locality 3020). In the plot, the *K* parameter measurements made using an MKF–1FB instrument are shown with a solid line, those made with a KT–10 instrument are shown by a dashed one: *1*, the boundaries of the petromagnetic complexes; *2*, the boundaries of the Units; the other symbols are the same as in Fig. 2.

greenish clays (Fig. 3, 5); the thickness of the latter notably increases up the section.

The overlying lithologically homogeneous clay–silty beds (Units 6–10), which rests upon the erosion

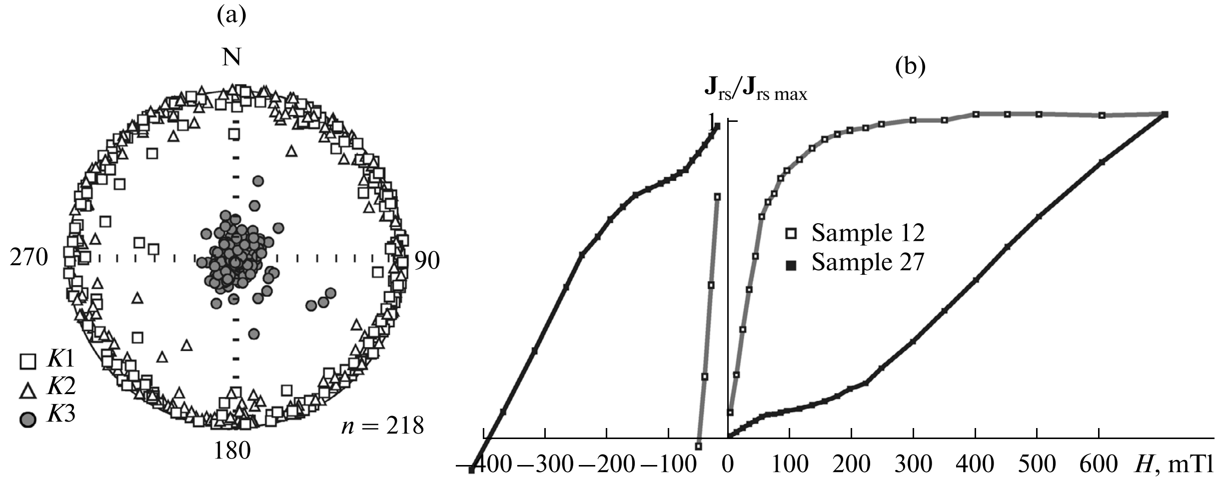

Fig. 5. The distribution of the axes of the ellipsoids of the magnetic susceptibility (a) and curves of magnetic saturation–elimination (b).

surface (a fact that is not accepted by all of the other researchers) and with another erosion surface covered by the Sangryk Beds also corresponds to an independent stage of basin evolution. We ascribe it to the Tolagaysor Formation. Hence we consider the formation in the same sense as King et al. (2013). As well, we use the name Sangryk Beds after King et al. (2013) conditionally, since earlier in the Utvinsk–Khobdinsk District this interval was included in the Shubarsay Formation (Beniamovskiy, 1994). Undoubtedly, this problem requires further attention.

Biostratigraphic Studies

A large body of information on the biostratigraphic characteristic of the studied section has been accumulated (Beniamovskiy et al., 1990; Zhelezko and Kozlov, 1999; Steurbaut, 2011; King et al., 2013). The most detailed data on the distribution in the section of dinocysts, nanoplankton, foraminifers, ostracods, pteropods, selachii, and other fossils were published by King et al. (2013). These data are summarized in Table 2.

According to the biostratigraphic data in the bottom of the section a gap was recognized: it lasted for the entire Paleocene, thus, Units 1–10 correspond practically to the entire Ypresian. The hiatuses at the boundaries of the majority of other Units within the interval are insignificant. At the boundary between Unit A1 and Unit A2 a hiatus that corresponds to two dinocyst zones (Wetzeliella astra and W. meckelfeldensis) was recognized. As well, a significant gap was found between Units 10 and 11 (C2 and D after King et al., 2013), the age of the latter corresponds to the Late Lutetian–Early Bartonian Stages (Beniamovskiy, 1994; King et al., 2013). The overlying Units 12 and 13 (the Sarmatian Stage of Miocene) also occur with a significant hiatus. Note, that Units 11–13 have not been studied in detail and the thickness of the sediments, according to various researchers, is different.

Petromagnetic Studies

During the petromagnetic studies the following parameters were acquired (Fig. 4): K is the magnetic susceptibility, whose magnitude is determined by concentrations of para-and ferromagnetic minerals in a rock (it is suggested that values of $K > 20 \times 10^{-5}$ SI units are caused by ferromagnetic minerals only); K_t, is the magnetic susceptibility, acquired after rock heating at 500°C for 1 hour. The increment of $dK = K_t–K$ reflects concentration of finely dispersed pyrite in a sample caused by phase transition of FeS_2 to highly magnetic Fe_3O_4 at a temperature above 400°C (Burov and Yasonov, 1979). As well, J_N was measured, which is the natural residual magnetization, whose module depends on the concentration of ferromagnetic minerals only and also on the degree of regularity of their magnetic moments. Thus, the values of J_N may substantially differ even for equal concentrations of ferromagnetics. J_{RS} is the residual magnetization of saturation, which is the maximal possible residual magnetization in a sample created by an artificial magnetic field. Its magnitude is influenced by the concentrations and grain sizes of ferromagnetics. The H_{CR} parameter is the residual coercive force that should be applied to completely eliminate the J_{RS} of a sample. It depends on the magnetic rigidity of a carrier of magnetism (magnetically soft are minerals such as magnetite, while iron hydroxide and hematite are magnetically hard).

The anisotropy of the magnetic susceptibility (AMS) or magnetic texture is a parameter of the magnetic susceptibility of a rock, measured in different directions. Various types of magnetic anisotropy are indicators of the hydrodynamic regime. In this case

Table 1. The evolution of opinions on the stratigraphic subdivision of the studied key section

<table>
<tr><th colspan="2">(Beniamovskiy et al., 1990)</th><th colspan="2">(Zhelezko and Kozlov, 1999)</th><th colspan="3">(King et al., 2013)</th><th colspan="4">Our data</th></tr>
<tr><th>Stage, substage</th><th>Forma-tion</th><th>Series, stage, substage</th><th>Forma-tion</th><th>Stage, substage</th><th>Formation</th><th>Unit</th><th>Stage, substage</th><th colspan="2">Formation, sub-formation, bed</th><th>Unit</th></tr>
<tr><td rowspan="2">Sarmatian</td><td rowspan="2"></td><td>Miocene</td><td></td><td>Sarmatian</td><td>“Sarmatian”</td><td></td><td>Sarmatian</td><td colspan="2"></td><td>12–13</td></tr>
<tr><td rowspan="5">Lutetian</td><td></td><td>Upper Lutetian–Bartonian</td><td>Sangryk?</td><td>D</td><td>Upper Lutetian–Bartonian</td><td colspan="2">Sangryk</td><td>11</td></tr>
<tr><td rowspan="6">Upper Lower Eocene–lower Middle Eocene</td><td rowspan="6">Tolagaysor</td><td rowspan="7">Tolagaysor</td><td rowspan="10">Ypresian</td><td rowspan="5">Tolagaysor</td><td rowspan="4">C2</td><td rowspan="10">Ypresian</td><td colspan="2" rowspan="5">Tolagaysor</td><td>10</td></tr>
<tr><td>9</td></tr>
<tr><td>8</td></tr>
<tr><td>7</td></tr>
<tr><td rowspan="6">Ypresian</td><td>C1</td><td>6</td></tr>
<tr><td rowspan="2">Aktulagay</td><td>B2</td><td rowspan="5">Alashen</td><td>Upper</td><td>5</td></tr>
<tr><td rowspan="4">Lower part of the Lower Eocene</td><td rowspan="4">Alashen</td><td>B1</td><td rowspan="3">Middle</td><td>4</td></tr>
<tr><td rowspan="3">Alashen</td><td rowspan="3">Alashen</td><td>A3</td><td>3</td></tr>
<tr><td>A2</td><td>2</td></tr>
<tr><td>A1</td><td>Lower</td><td>1</td></tr>
</table>

Unit with the thickest layer of sapropelite.
* Here and further a member with the thickest sapropelite beds is highlighted in gray.

short axes of magnetic ellipsoids ($K3$) are concentrated in the center of a stereogram, while the long ($K1$) and medium ($K2$) axes are equally distributed along its equator (Fig. 5a); this picture is typical for sediments that were deposited in a calm hydrodynamic environment.

Apart from the characteristics measured by experimental work, the following parameters were calculated: The Q factor (the Koenigsberger parameter) is the ratio of the natural residual magnetization against the inductive magnetism; as well, the parameter of magnetic rigidness $S = J_{R(-300)}/J_{RS}$, where $J_{R(-300)}$ is the residual magnetism after the effect of a 300 mTl magnetic field, and the parameter K/J_{RS} (Fig. 4). The values of the Q factor > 1 in sedimentary rocks as a rule suggest a chemical nature of magnetism. The magnitudes of the S parameter that are near zero are indicators of hematite (Evans and Heller, 2003). The K/J_{RS} ratio characterizes the average size of ferromagnetic mineral grains.

Curves of saturation have been obtained for 13 samples (Fig. 5b), which allowed the recognition of a magnetically soft phase (sample 12): J_{RS} was induced under the effect of a magnetic field of 250–350 mTl, which is typical for finely dispersed magnetite or similar minerals. As well, a rigid magnetic phase (sample 27) was detected: its saturation was not reached even at 700 mTl, which suggests the presence of hematite or iron hydroxides.

Measurements of K in the field were carried out using portable KT–6 and KT–10 instruments, as well as in the laboratory with an MFK1–FB kappabridge and residual magnetism was found with a dual-speed JR–6 spinner magnetometer. Hysteresis characteristics (J_{RS}, J_r and H_{CR}) were acquired with a controllable electric magnet with a maximum field strength of 700 mTl (in cases where saturation was not reached, the magnetization that was induced after application of a 700 mTl field was taken instead of J_{RS}). The dK parameter was measured after heating of samples in an SNOL–6/11–V furnace. The anisotropy analyses were carried out using Anysoft 4.2 software. The results of field and laboratory measurements of K demonstrated a good fit (Fig. 4).

The studied section is pronouncedly subdivided into three petromagnetic complexes (PC) (Fig. 4).

The lowermost PC1 complex is characterized by high variability of K and minimal J_N, along with a low (with a few singular exceptions) and generally decreasing upward in the section J_{RS}, a wide scatter of K/J_{RS} on the background of a certain trend of the growth of average values upward in the section and the presence of minimal values of S and maximal H_{CR} and dK.

Within the limits of the PC2 the values of K and H_{CR}, with the exception of single levels, are quite homogeneous, the values of J_N, J_{RS} and S are at a maximum, K/J_{RS} is at a minimum, some levels with anomalously high dK were found, which, however, in abso-

Table 2. Stratigraphic subdivision of the studied key section

Stage, substage	(King et al., 2013) unit	(King et al., 2013) formation	Our data: formation, sub-formation, bed		Our data: unit	Our data: PC*	Zones (King et al., 2013; Beniamovskiy et al., 1990; Beniamovskiy et al., 1994; Zhelezko and Kozlov, 1999): Nanno-plankton	Dinocysts	Selachii	Foraminifers: planktonic	Foraminifers: benthic	Ptero-pods
Sarmatian		"Sarmatian"			12–13							
Upper Lutetian–Bartonian	D	Sangryk?	Sangryk		11	3		Rhombodinium draco (in the bottom)				
Ypresian	C2	Tolagaysor	Tolagaysor		10	2	NP14a	Wetzeliella eocaenica	Otodus auriculatus auriculatus (E10)	E7–E8?	Uvigerina bykovae	
					9						Bulimina praeinflata	
					8							
					7							
	C1				6		NP13	Areosphaeridium diktyoplokum	Otodus auriculatus disauris (E9)			
	B2	Aktulagay	Alashen	Upper	5	1	NP12				Bulimina mitgarziana	9b
								Charlesdowniea coleothrypta				9a
	B1**			Middle	4**							
	A3	Alashen			3			Dracodinium varielongitudum	Otodus aksuaticus (E8)	E5 and or older	Pseudogaudryina externa	8/9
					2							
	A2			Lower	1		NP11	Eatonicysta ursulae				
								Dracodinium simile				
	A1						NP10b	Deflandrea oebisfeldensis				

* PC petromagnetic complexes. ** Unit with thw thikest layer of sapropelite.

lute values are considerably lower, than similar occurrences in PC1.

PC3 is characterized by the highest values of K and K/J_{RS}, with low J_N and J_{RS}, as well as decreased H_{CR} and constantly high S and elevated dK.

Each of the PCs correspond to a large stage of the paleobasin evolution, since petromagnetic variations are caused by sediment rhythmicity, which is connected by variations of sea level and changes of geochemical environments in sediments (Guzhikov, Molostovsky, 1995). Thus, levels of abrupt changes of the magnetic properties along with lithologic and sedimentary features are objective criteria for subdivision of the sections into formations. Thus, PC1, PC2, and PC3 correspond to the Alashen and Tolagaysor Formations and the Sangryk Unit, respectively (Fig. 4). PC1 is additionally split into two parts, viz., a lower one with elevated J_{RS} and J_N and an upper one with decreased J_{RS} and J_N, which are higher in the average values of K/J_{RS} and anomalous S, H_{CR} and dK (Fig. 4). The boundaries between these parts are located at the base of Unit 3, corresponding to a substantial increase of anoxic conditions and from the point of view of petromagnetism this is more significant in the sense of geological events than lithologic boundaries that mark the bases of Units 2 and 4.

The Environments of the Sedimentary Basin Formation

Based on the data that were obtained, several stages of basin evolution are recognized. According to King et al. (2013) the studied section may be divided into four sedimentary sequences. We have not recognized the lowermost one (20 cm at the base of Unit 1, after King et al., 2013). It has been proposed on the grounds of paleontological data and additionally proven by phosphorite concentration. We may admit the possibility of its existence, since in this part of the section the sediments are strongly condensed. According to our observations, the phosphorites of Unit 1 are dispersed in the lower 15–20 cm and penetrate into the underlying layers for 20–30 cm through *Thalassinoides* burrows (Figs. 4, 7). It cannot be ruled out that this is an older (Paleocene or Late Cretaceous?) system of burrows that were dug through for the second time. In the latter case, even the existence of several sequences in that part of the section may be allowed.

The second sequence after King et al. (2013) corresponds to the major part of Unit 1 along with Units 2–5, i.e., to the interval of PC1. Units 1–3 contain numerous levels with *Chondrites* and *Pilichnus*, which mark short interruption of the sediment accumulation and development of anoxic conditions (a total of 14, according to the data by King et al., 2013). The characteristic feature of this interval is the scarcity of macro-benthic faunas and the moderate biodiversity of benthic foraminifers and ostracods, as well as the alternation of sub-intervals of sediments that were bioturbated by *Chindrites* and *Pilichnu*s that could sustain anoxia with layers of finely laminated and horizontally bedded clays without traces of bioturbation. The proportion of the latter increases upwards simultaneously with the appearance of darker and brown sediment colors. Apparently, these phenomena are interconnected and caused by the growth of oxygen deficiency in the sediments (Bromley, 1996). While Unit 1 is dominated by large *Chondrites* (of the *targionii* group) and *Pilichnus* (Figs. 3, 4), along with the presence of *Zoophycos* (King et al., 2013), Units 2 and 3 bear small *Ch. intricatus* and *Pilichnus*. Unit 4 contains no *Chondrites* and its section is represented by undisturbed finely laminated sapropelite and clays, which suggests strongly anoxic environments. This conclusion is supported by the practically complete disappearance of benthic faunas (ibid.) and high concentrations of finely dispersed pyrite, which, in turn is reflected in anomalous values of dK within the interval of Units 3–5 (Fig. 4). This part of the section is the most condensed, which is typical for the majority of sapropel horizons (Baraboshkin, 2009). Unit 5, in general, is similar to Unit 3, but differs from the latter in the absence of large *Chondrites* (Fig. 3, 4) and the presence of true sapropelite. It is also condensed, but has been accumulated with more interruptions of sedimentation, which led to partial destruction of the organic matter and phosphorite formation. The Unit 3–5 interval is also notable due to high pyrite content and the presence of hematite and iron hydroxides (which is determined by a minimum of S and maximum of H_{CR} parameters); the latter two are probably oxidation products after pyrite.

Hence, Units 1–5 form a singular sequence that accumulated in an open-sea environment under the influence of variable oxygen concentrations in the sediments. The surface of the maximum sea level in the sequence is apparently located within the thickest sapropel layer (Unit 4). Consequently, the evolution of anoxic conditions in the studied area was under the control of eustatic fluctuations. The sapropelite formation could be caused by an inflow of cold waters from the West Siberian Basin through the Turgay Strait (Fig. 6a) (Beniamovskiy, 2007; King et al., 2013): the latter event triggered plankton productivity.

The following third sequence corresponds to Units 6–10 and PC2, which coincides with the opinion of King et al. (2013). These deposits formed at a shallower depth with higher input of clastic materials, which is supported by the presence of silt and sands in the sequence, along with presence of flow-ripple marks at the base of Unit 6. At the same time the sequence has dominant horizontal bedding, bioturbation traces are occasional, while complexes of benthic and plankton microfaunas indicate open-sea environments with normal sediment aeration (ibid.). The combination of these features suggests a relatively shallow-water basin, yet below the wave basis, and a sharp increase of sedimentation rates. The sequence finishes with the sea level lowering and formation of a regional hiatus surface (Beniamovskiy, 2007). It is

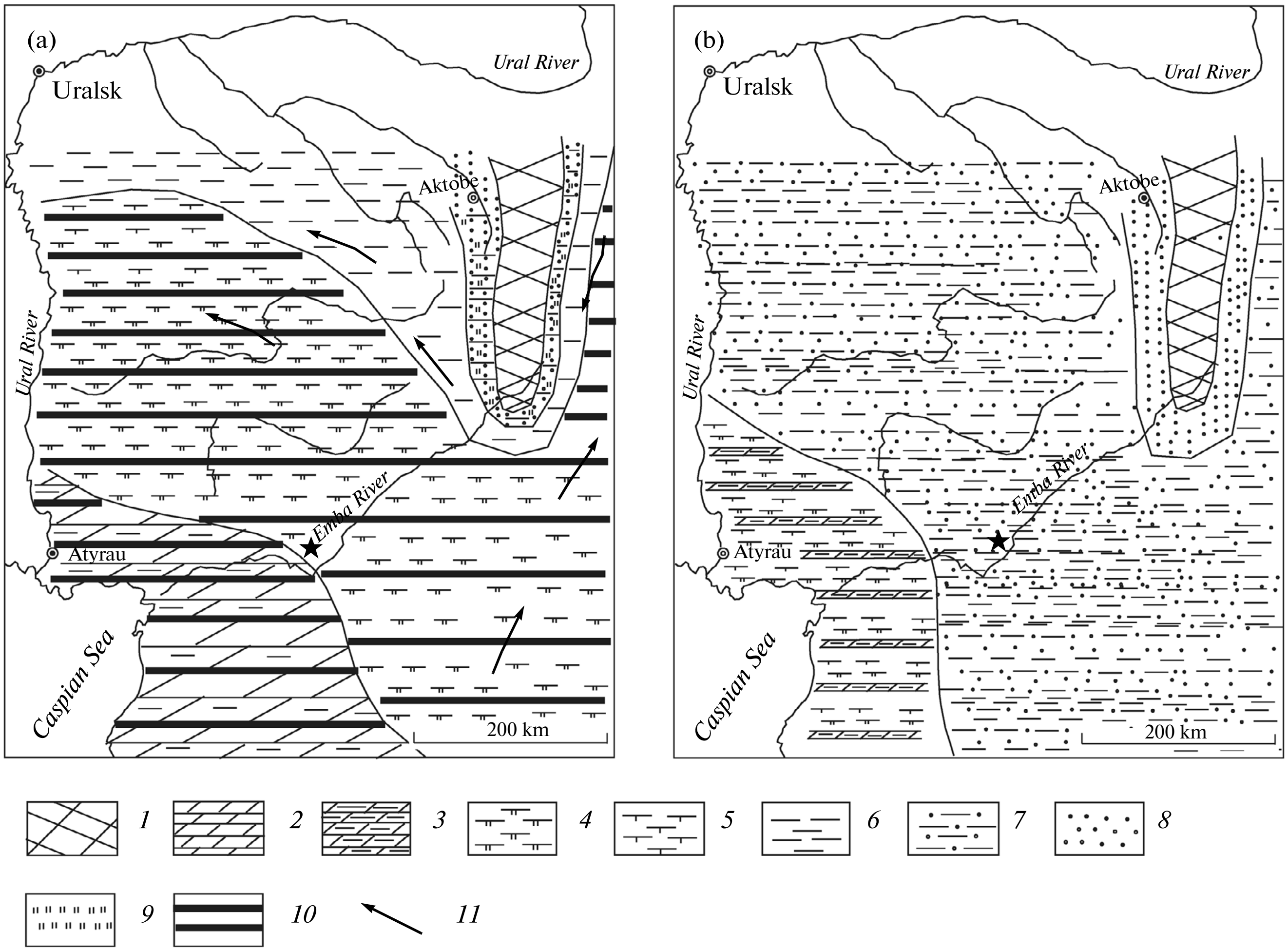

Fig. 6. Lithologic, palaeogeographic schemes after Beniamovskiy (1994) with additions: (a) Early Ypresian (the Alashen Time), (b) Late Ypresian (the Tolagaysor Time); *1*, erosion area; *2–9*, sea deposits: *2*, marls; *3*, clayey marls; *4*, highly calcareous clays; *5*, calcareous clays; *6*, non-calcareous clays; *7*, sand-bearing and silty clays, clayey silts; *8*, sands sandstones and silts; *9*, siliceous clays, rottenstone and diatomite; *10*, sapropels (bituminous shales); *11*, system of surficial currents, after Beniamovskiy (2007). The asterisk shows the location of the studied key section.

notable that during the third sequence (Late Ypresian–Early Lutetian) a fundamental re-structuring of the water circulation system took place, as has been found in the Northeast Peri-Caspian, (westward off the Ural River to the Mugodzhar Hills) and in the South Turgay Depression (Beniamovskiy et al., 1993; Beniamovskiy, 1994; Figs. 30 and 32). Due to regression in the West Siberian Basin and its seclusion from the Arctic Ocean (Yakovleva and Aleksandrova, 2013, Fig. 5) the inflow of cold water masses ceased, causing in turn an abrupt drop in plankton productivity, which is required for sapropel formation (Fig. 6b). From the point of view of petromagnetics the third sequence is very homogeneous (Fig. 4), which indirectly agrees with the idea of high sedimentation rates. The sharp increase of the J_N, Q, and J_{RS} parameters in comparison with PC1 and simultaneous fall of K/J_{RS} (Fig. 4) prove that changes occurred in the composition and grain size of the ferromagnetic fraction (and a possible change in genesis from authigenic to allothigenic).

Finally, the fourth sequence corresponds to the Sangryk Beds (Unit 11 and PC3); it is built of finely laminated anoxic bituminous shales. Petromagnetically, Unit 11 is similar to the interval of Units 3–5 of the second sequence (Fig. 4). Judging by the saturation with sulfides, as indicated by the dK high values (Fig. 4) the degree of anoxic conditions in the shales was similar or even higher than that in Unit 4. Unfortunately, there is still not enough data to explain the possible mechanism of formation of this slate. These rocks aren't disturbed by bioturbation, which suggests that they were accumulated below the wave basis under anoxic conditions; apart from this, the upper part of the shales has clear traces of landslide deformations, which suggests the existence of a slope during sedimentation or somewhat later.

CONCLUSIONS

Thus, these studies allowed us to achieve the following results:

(1) The knowledge on the section's structure became more accurate;

(2) The volumes of the Tolagaysor and Alashen Formations were revised and the latter one was subdivided into three parts. Recognition of the Aktulagay Formation has been demonstrated to be incorrect;

(3) For the first time, the detailed petromagnetic characteristic of the section was obtained.

The conducted sedimentologic studies of the section proved the correctness of the recognition of four sequences, which also is supported by the petromagnetic data. The Alashen Formation corresponds to the first and second sequences, or PC1 (Units 1–5); the Tolagaysor Formation encompasses the third sequence, or PC2 (Units 5–10); the Sangryk Beds corresponds to the fourth sequence and PC3 (Unit 11).

ACKNOWLEDGMENTS

We are grateful to T.R. Akopov and K.E. Knizhnik (from LLP Zaprudgeologiya, Aktube, Kazakhstan) for help during the field work and the drivers from this partnership, Yu.A. Dergach and V.A. Dimitriev.

The study has been carried out with financial support of the RFBR (grants no. 12-05-00196-a, 13-05-00745-a and 14-05-00421) and Ministry for Education and Science of Russia within framework of base part (state registration no. 1140304447, project code 1582) and state request in area of Scientific activities (assignment no. 17557) as well as project no. 28 of teh Presidium of RAS.

REFERENCES

Baraboshkin, E.Yu., Condensed sections: terminology, types, and accumulation conditions, *Moscow Univ. Geol. Bull.*, vol. 64, no. 3, pp. 153–160.

Benyamovsky, V.N., Segedin, R.A., Akopov, T.R., et al., New Paleocene and Eocene formations of the Caspian Basin, *Byull. Mosk. O-va Ispyt. Prir., Otd. Geol.*, 1990, vol. 65, no. 5, pp. 68–76.

Benyamovsky, V.N., Vasil'eva, O.N., Levina, A.P., and Pronin, V.G., Paleogene of the Southern Trans-Urals, Paper 1: Paleogene in the southern part of the Turgay Trough, *Izv. Vyssh. Uchebn. Razved., Geol. Razved.*, 1993, no. 6, pp. 22–36.

Benyamovsky, V.N., Stratigraphic scheme for the Paleogene of the Caspian-Mugodzhary Region as an example of creating the regional stratigraphic scheme for Paleogene based on paleogeographic data, in *Paleogeograficheskoe obosnovanie stratigraficheskikh postroenii* (Paleogeographic Substantiation of Stratigraphic Schemes), Moscow: Izd. Moscow State Univ., 1994, pp. 90–120.

Benyamovsky, V.N., Paleogene longitudinal straits of the Northern Eurasia, in *Prolivy Severnogo polushariya v melu i paleogene* (Straits of the Northern Hemisphere in Cretaceous and Paleogene), Moscow: Izd. Moscow State Univ., 2007.

Bromley, R.G., *Trace Fossils. Biology, Taphonomy, and Applications, 2nd ed.*, L.: Chapman, 1996.

Burov, B.V. and Yasonov, P.G., *Vvedenie v differentsial'nyi termomagnitnyi analiz gornykh porod* (Introduction in Differential Thermomagnetic Analysis of Rocks), Kazan: Izd. Kazan State Univ., 1979.

Droser, M.L. and Bottjer, D.J., A semiquantitative field classification of ichnofabric, *J. Sed. Petrol.*, 1986, vol. 56, no. 4, pp. 558–559.

Evans, M.E. and Heller, F., *Environmental Magnetism: Principles and Applications of Enviromagnetics*, Elsevier: Acad. Press, 2003.

Geologiya SSSR. T. XXI. Zapadnyi Kazakhstan. Ch. I. Geologicheskoe opisanie. Kn. 1 (Geology of the USSR. Vol. XXI. West Kazakhstan. Part I. Geological Description. Book 1), Moscow: Nedra, 1970.

Guzhikov, A.Yu. and Molostovskii, E.A., Stratigraphic information value of numerical macnetic characteristics of sedimentary rocks (aspects of methodology), *Byull. Mosk. O-va Ispyt. Prir., Otd. Geol.*, 1995, vol. 70, no. 1, pp. 32–41.

King, C., Iakovleva, A., Steurbaut et al., The Aktulagay Section, West Kazakhstan: a key site for northern mid-latitude Early Eocene stratigraphy, *Stratigraphy*, 2013, vol. 10, no. 3, pp. 171–209.

Koltypin, S.N., Upper Cretaceous deposits of the Ural--Emba Salt Dome, the southwestern Cis-Urals and Mugodzhary region), in *Tr. VNIGRI* (Proc. All-Russ. Petroleum Res. Explor. Inst.), Leningrad: Nedra, 1957.

Malyshkina, T.P., *Elasmobrankhii zapadnoi okrainy Zapadno-Sibirskogo paleogenovogo basseina* (Elasmobranchs of Western Marginal Area of the West Siberian Paleogene Basin), Yekaterinburg: IGG UrO RAN, 2006.

Steurbaut, E., New calcareous nannofossil taxa from the Ypresian (Early Eocene) of the North Sea basin and the Turan Platform in West Kazakhstan, *Bull. Inst. Roy. Sci. Nat. Belgique. Sci. de la Terre*, 2011, vol. 81, pp. 247–277.

Iakovleva, A.I. and Aleksandrova, G.N., The problem of dinocyst zonation of the Paleocene–Eocene deposits of Western Siberia, *Byull. Mosk. O-va Ispyt. Prir., Otd. Geol.*, 2013, vol. 88, no. 1, pp. 59–81.

Zhelezko, V.I. and Kozlov, V.A., Elasmobranchii and Paleogene biostratigraphy of Trans-Urals and Central Asia, in *Materialy po stratigrafii i paleontologii Urala* (Materials on Stratigraphy and Paleontology of the Urals), 1999, no. 3.

Translated by A. Larionov